

# BUBBLE REMOVAL FROM GLASS MELTS WITH SLOW VERTICAL CIRCULATIONS

#MARCELA JEBAVÁ, LUBOMÍR NĚMEC

Laboratory of Inorganic Materials, Joint Workplace of the Institute of Chemical Technology Prague,  
Technická 5, 166 28 Prague 6, and the Institute of Inorganic Chemistry AS CR, v.v.i., 250 68 Řež, Czech Republic

#E-mail: majebava@vscht.cz

Submitted April 24, 2011; accepted July 3, 2011

**Keywords:** Bubbles, Glass-melt circulation, Pot furnace, Mathematical modelling, Fining efficiency

*A simple model of bubble behaviour in a melting space with a vertical circulation of the molten glass was derived. Subsequently, two cases were considered. The first case with a constant, radially independent value of the angular velocity of the glass-melt rotation approximately demonstrated the heating through the wall of the pot furnace for glass melting, and the second case, where the angular velocity decreased from the centre of the space towards the wall, represented the heating of the pot furnace from above. The chosen values of the angular velocities corresponded to temperature gradients commonly occurring in melting spaces. The starting positions of critical (last removed) bubbles were sought along with their trajectories and fining times. The much higher calculated fining times of critical bubbles in the rotating melt as compared with the fining times of the bubbles just rising through the quiescent glass melt were explained by the deceleration of the bubble rising with respect to the fixed coordinates through the downward part of the glass vertical circulation. This fact leads to a long retention of the bubble in the melt and consequently to high energy consumption and low melting performance. The semiempirical equations were presented, providing the fining time of the critical bubble as a function of the bubble-growth rate and melt-rotation velocity.*

## INTRODUCTION

The removal of small bubbles from viscous liquids in a gravitational field is always problematic. Bubble-rise velocity in viscous liquids is considerably low, the liquid layers often thick and the flow patterns, if present, may also slow the average bubble-rise velocity [1-4]. Similar problems may be observed when a small amount of liquid or solid particles is settling. In previous works [5-8], the authors have dealt with the impact of glass-flow character on bubble removal in a continuous glass-melting channel and found both beneficial and disadvantageous types of the natural glass flows in terms of the bubble removal process. In the discontinuous pot furnace, the glass-melt flow is determined by the radial temperature gradients between the pot wall and the inside. The circulations with the upward flow in the centre of the pot are caused when the temperature decreases from the space centre to the wall, and the opposite flow is induced when the temperature is higher near the wall. The mentioned circulations resemble the transversal glass circulations set in the horizontal channel, where the bubble should pass a part of its trajectory against the downward glass flow and its rising to the level is thus hindered [5-6]. This work is focused on the mathematical modelling of small bubbles in the mentioned circulation field in the

glass-pot furnace with the aim of elucidating the relation between the fining efficiency, melt circulation intensity, and bubble-growth rate. A special simplified model has been derived for the purpose of this modelling.

## THEORETICAL

A new quantity called utilisation of the melting space has been introduced in a previous work to evaluate quantitatively the impact of glass-flow character on the dissolution of sand grains and the removal of bubbles [6]. The utilisation of the space for the process of the bubble removal in discontinuous space may be simply expressed as the ratio between the critical bubble-fining time in the space with quiescent molten glass and the corresponding time in the same space with flow patterns of the glass or by the ratio of the appropriate fining heights:

$$u = \frac{\tau_{Fref}}{\tau_{Fcrit}} \doteq \left( \frac{h_0}{h_{virt}} \right)^{1/3}; \quad u \in \langle 0; 1 \rangle \quad (1)$$

where  $u$  is the space utilisation,  $\tau_{Fref}$  is the critical fining time in the quiescent glass,  $\tau_{Fcrit}$  is the same time in the space with flow patterns,  $h_0$  is the thickness of the glass layer and  $h_{virt}$  is the height to which the critical bubble

should rise to reach the glass level with respect to the melt. The critical fining time designates the maximum fining time of the smallest (critical) bubble in the space. Both quantities in the fraction of Equation (1) are obtainable by a simple calculation ( $\tau_{Fref}$ ) and by using the mathematical model ( $\tau_{Fcrit}$ ). The value of  $\tau_{Fref}$  of very small bubbles can be calculated from the following equation [5]:

$$\tau_{Fref} = \left( \frac{27h_0\eta}{2g\rho\dot{a}^2} \right)^{1/3} \quad (2)$$

where  $\eta$  and  $\rho$  are the glass viscosity and density and  $\dot{a}$  is the bubble-growth rate.

If the melt circulates, the critical fining time  $\tau_{Fcrit}$  may be obtained from an equation analogical to Equation (2) but the value of  $h_0$  is replaced by  $h_{virt}$ .

The bubble fining times of small bubbles in a quiescent or vertically rotating viscous liquid may generally be derived from several cases:

The liquid is quiescent,  $\omega = 0$ :

- a) if  $\dot{a} = 0$ ,  $\tau_{Fcrit} = 9\eta h_0 / 2g\rho\dot{a}_0^2$
- b) if  $\dot{a} > 0$ , equation (2) is valid.

The liquid is rotating,  $\omega > 0$ :

- a) if  $\dot{a} = 0$ , the ratio  $\omega/v_{bub}$  is significant where  $v_{bub}$  is the bubble rising velocity:
  - if  $\omega/v_{bub}$  is sufficiently small,  $\tau_F$  has a high but limited value,
  - if  $\omega/v_{bub}$  is sufficiently large,  $\tau_F \rightarrow \infty$ .
- b) if  $\dot{a} > 0$ , equation (2) is valid, where  $\tau_{Fref}$  is replaced by  $\tau_{Fcrit}$  and  $h_0$  by  $h_{virt}$ .

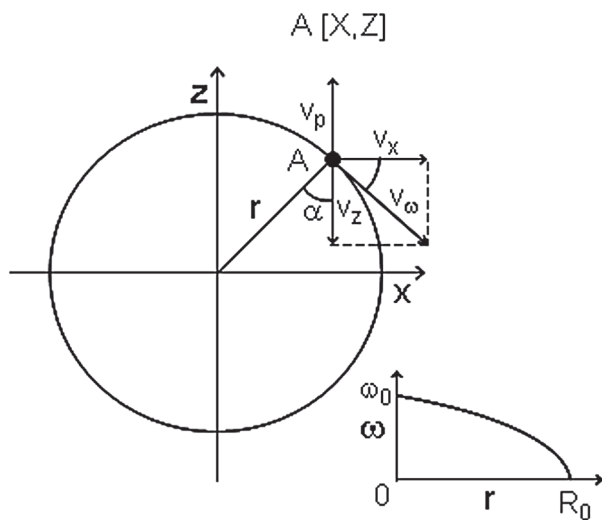


Figure 1. A schematic view of bubble A in the circular field of the glass melt. The detail shows the parabolic decrease of the angular velocity with the growing radius of the circle; X, Z – the bubble orthogonal coordinates,  $v_x$ ,  $v_z$  – the velocity components of the melt,  $v_\omega$  – the circumference velocity of the melt,  $v_p$  – the vertical velocity of the bubble,  $r$  – the radial distance,  $\alpha$  – the rotation angle,  $\omega$  – the clockwise angular velocity of the melt.

The most frequent cases of bubble behaviour in glass are growing bubbles, i.e. the case 2b for bubbles in a vertically rotating melt (natural circulation).

The spatial velocity field in the pot furnace may be replaced by a 2D picture of the vertical central section through the space. When deriving the simplified model of bubble behaviour, the circular glass-rotation field of the melt and the bubble ascending through the melt according to the Stokes' law are considered. The bubble grows linearly which corresponds well to the results of the experimental observations. The bubble behaviour in the circularly rotating melt is schematically depicted in Figure 1. Thus, the cylindrical space of the pot furnace is substituted by the vertical circular space with a radius of  $R_0$ .

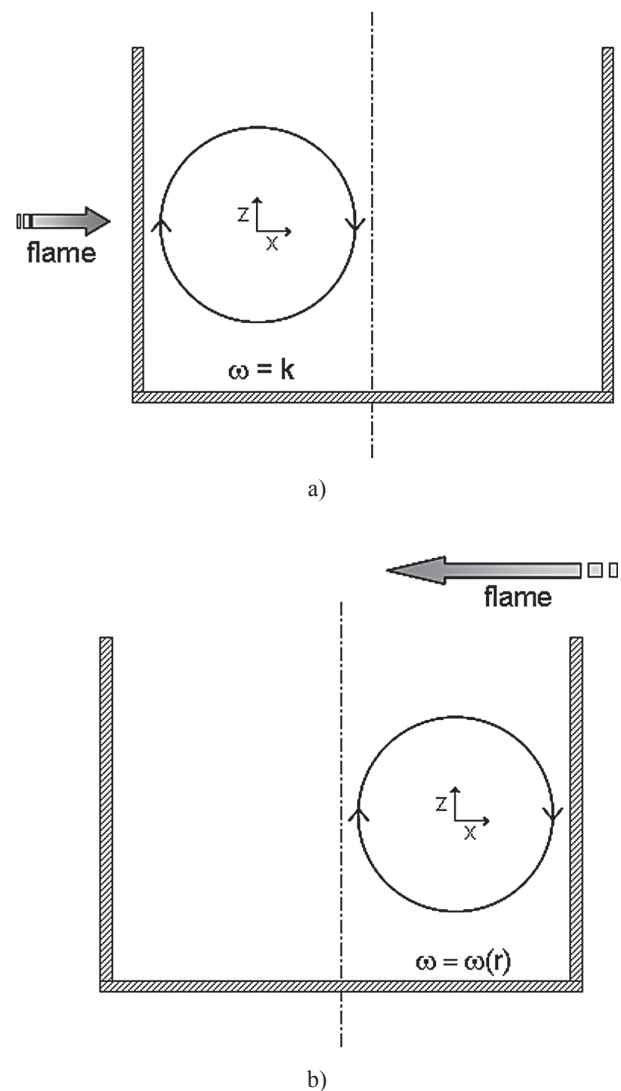


Figure 2. Two cases of the melt circulation in the pot furnace for the glass melting. a) the heating through the wall approximately characterised by the constant angular velocity of the melt; b) the heating from above approximately characterised by the angular velocity of the melt decreasing towards the pot wall. The downward part of melt circulation is important for bubble rise.

Two cases were considered: the case using the constant value of the melt angular velocity independent from the radius approximately describes the case with a higher temperature near the pot wall (heating through the wall), whereas the case with the angular velocity decreasing with radial coordinate towards the wall represents the case of temperature maximum in the centre of glass level (heating from above). Figure 2 presents both cases, where the left part represents heating through the wall and the right part shows heating from above. The downward part of the melt circulation is substantial for bubble rise, because the bubble spends more time in the downward flow than in the upward flow. Consequently, the case with downward circulation in the vertical axis of the pot - not hindered by pot walls - approximately simulates the case of heating through the pot wall, and the case with the downward flow close to the pot wall simulates heating from above.

The components of the glass-melt velocity are described by the following equations:

$$\begin{aligned} v_x &= v_\omega \cos \alpha = v_\omega \cos (\alpha_0 + \omega \tau) \\ v_z &= -v_\omega \sin \alpha = -v_\omega \sin (\alpha_0 + \omega \tau) \end{aligned} \quad (3a, b)$$

where  $v_\omega$  is the circumferential velocity of the melt,  $\omega$  is the angular velocity of the melt, and  $\alpha_0$  is the initial angle in time  $\tau = 0$ . Then:

$$\alpha_0 = \arcsin \frac{X_0}{\sqrt{(X_0^2 + Z_0^2)}} \quad (4)$$

where  $X_0$  and  $Z_0$  are the initial coordinates of the bubble, hence its starting position.

The circumference velocity of the melt is given by:

$$v_\omega = \omega r = \omega (X^2 + Z^2)^{1/2} \quad (5)$$

After the substitution of equation (5) into (3a, b):

$$\begin{aligned} v_x &= \omega (X^2 + Z^2)^{1/2} \cos (\alpha_0 + \omega \tau) \\ v_z &= -\omega (X^2 + Z^2)^{1/2} \sin (\alpha_0 + \omega \tau) \end{aligned} \quad (6a, b)$$

The bubble-rise velocity is given by the Stokes' law:

$$v_p = \frac{2g(\rho_l - \rho_p)(a_0 + \dot{a}\tau)^2}{9\eta} \quad (7)$$

where  $\rho_l$  and  $\rho_p$  are the densities of the liquid (melt) and particle (bubble), respectively,  $\eta$  is its viscosity,  $a_0$  is the initial particle radius, and  $\dot{a}$  is the particle growth or dissolution rate.

The elements of the bubble trajectory are then given by:

$$dX = v_x d\tau = \omega (X^2 + Z^2)^{1/2} \cos (\alpha_0 + \omega \tau) d\tau \quad (8a, b)$$

$$dZ = v_{pz} d\tau = \left[ -\omega (X^2 + Z^2)^{1/2} \sin (\alpha_0 + \omega \tau) + \frac{2g(\rho_l - \rho_p)(a_0 + \dot{a}\tau)^2}{9\eta} \right] d\tau$$

where  $v_{pz}$  is the resulting vertical velocity of the particle. The following equation is proposed for the angular melt velocity at radius  $r$  in the circular space with the final radius  $R_0$  (space boundary):

$$\omega = \omega_0 \left( 1 - \frac{r^2}{R_0^2} \right) = \omega_0 \left( 1 - \frac{X^2 + Z^2}{R_0^2} \right) \quad (9)$$

where  $\omega_0$  is the melt angular velocity in the circle centre. Equation (9) is substituted into Equations (8a, b):

$$dX = v_x d\tau = \omega_0 \left( 1 - \frac{X^2 + Z^2}{R_0^2} \right) (X^2 + Z^2)^{1/2} \cos \left( \alpha_0 + \omega_0 \left( 1 - \frac{X^2 + Z^2}{R_0^2} \right) \tau \right) d\tau \quad (10a, b)$$

$$dZ = v_{pz} d\tau = \left[ -\omega_0 \left( 1 - \frac{X^2 + Z^2}{R_0^2} \right) (X^2 + Z^2)^{1/2} \sin \left( \alpha_0 + \omega_0 \left( 1 - \frac{X^2 + Z^2}{R_0^2} \right) \tau \right) + \frac{2g(\rho_l - \rho_p)(a_0 + \dot{a}\tau)^2}{9\eta} \right] d\tau$$

Equations (10a, b) are solved numerically. When the bubble reaches the radial distance  $R_0$  in the upper half of the space, the calculation is completed, i.e. the bubble attains the glass level.

#### Calculation conditions

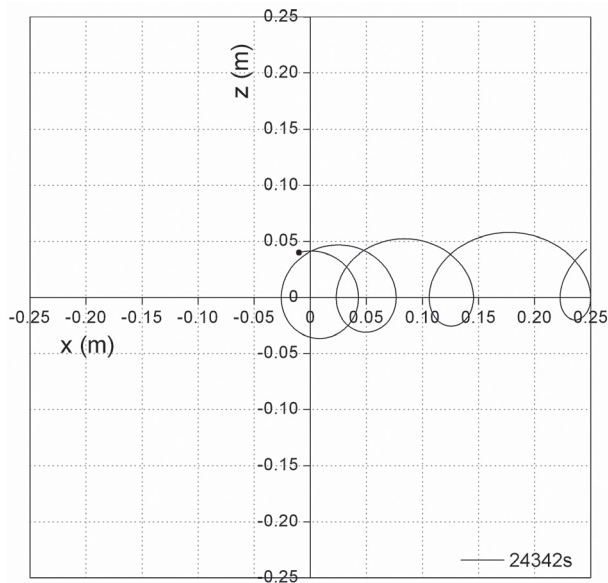
As already mentioned, the bubble behaviour in the space heated through the wall is simulated by the case with the angular velocity of the melt independent of the radial distance  $r$ , whereas glass heating from above is represented by the case with the value of the melt angular velocity decreasing towards the wall (according to equation (9)). The models are only an approximation of reality, but an important feature of the bubble behaviour is involved - the decisive part of the bubble rise takes place in the downward flow of the melt. The downward part of the melt-circulation flow is slowed down by the presence of the solid surface (pot wall) when the glass is heated from above, and no resistance is met in the pot centre when glass is heated through the wall.

The impact of the temperature gradient on the circulation intensity is simulated by the value of the initial angular velocity of the melt, which in reality increases with the value of the temperature gradient. The interval of  $\omega_0 \in \langle 10^{-3}; 10^{-2} \rangle$  (rad/s) corresponds to the values obtained by the modelling of the horizontal melting channel in the range of temperature gradients of 10-100°C/m [6]. The bubble-growth rate was chosen in the interval of  $10^{-8}$  to  $10^{-6}$  m/s. The choice is in agreement with the values of bubble-growth rates obtained by experiments with industrial glasses. The initial radius of the critical (smallest) bubble  $5 \times 10^{-5}$  m was chosen for the calculations; the glass-melt viscosity was 30.35 Pa s and glass density 2415 kg/m<sup>3</sup> (the model TV glass at 1300°C). The value of  $R_0$  was 0.25 m. The starting point of the critical bubble has been identified by repeated calculations of the fining time by using the regular mash of the starting points with the aim to find the critical coordinates. The values of  $\tau_{Fref}$  have been calculated from equation (2), where  $h_0 = 2R_0$ .

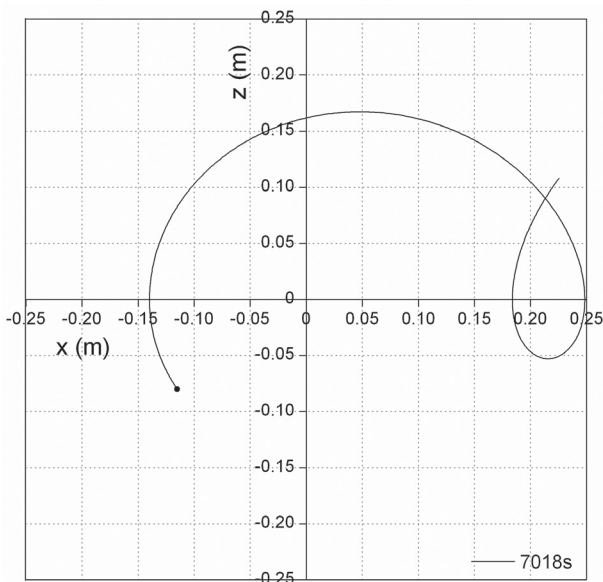
RESULTS OF CALCULATIONS

The typical critical bubble trajectories for the bubble-growth rates  $5 \times 10^{-8}$  and  $2 \times 10^{-7}$  m/s are presented in Figure 3. The bubbles draw spiral traces leading to the right and showing the growing radius with the increasing value of the bubble-growth rate. Both features are a natural result of the interaction of the circular and vertical movement. Figure 4 brings the calculated values of  $\tau_{Fref}$  and  $\tau_{Fcrit}$  for the case of a constant value of  $\omega$  ( $\omega = k$ , heating through the wall). The values of

$\tau_{Fcrit}$  were calculated for  $\omega_0 = 1 \times 10^{-3}, 2 \times 10^{-3}, 4 \times 10^{-3}$  and  $1 \times 10^{-2}$  rad/s. As arises from Figure 5, the positions of the starting points of the critical bubbles are located on the planar spiral, which opens as the value of the bubble-growth rate increases. When decreasing the melt rotational velocity, the starting points of the critical bubble should approach the lowest point of the circle with the radius  $R_0$ . The approximately hyperbolic decrease of fining times with increasing bubble-growth rate is clear in all of the cases; the fining times grow with the intensity of the melt circulation and in all of the cases are much higher than the values of  $\tau_{Fref}$ .



a)



b)

Figure 3. The typical critical trajectories of bubbles in the circular velocity field of the melt for the bubble-growth rates of: a)  $5 \times 10^{-8}$  and b)  $2 \times 10^{-7}$  m/s. The case of the constant value of  $\omega_0 = 10^{-3}$  rad/s (heating through the wall).

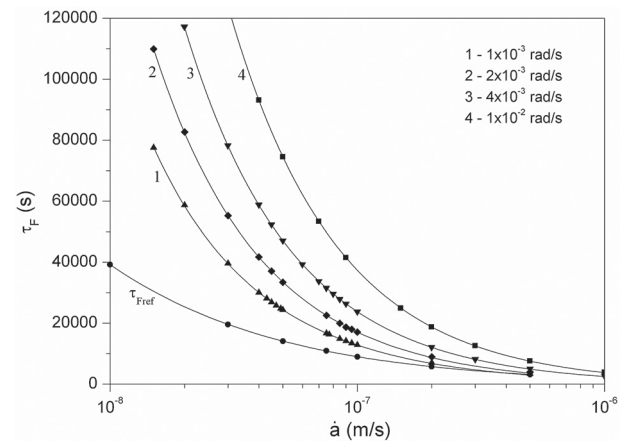


Figure 4. The calculated values of  $\tau_{Fref}$  and  $\tau_{Fcrit}$  for the case of a constant value of  $\omega = k$  (heating through the wall). The values of  $\tau_{Fcrit}$  were calculated for  $\omega_0 = 1 \times 10^{-3}, 2 \times 10^{-3}, 4 \times 10^{-3}$  and  $1 \times 10^{-2}$  rad/s.

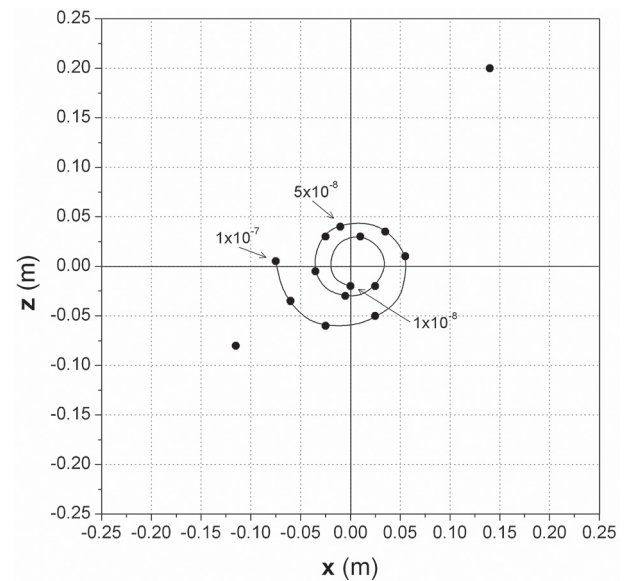


Figure 5. The positions of starting points of the critical bubbles as a function of values of the bubble-growth rates in the case of the constant value of  $\omega_0 = 10^{-3}$  rad/s (heating through the wall). The numbers close to the points are the values of the bubble-growth rates in m/s.

Similar results were acquired for the more frequent case of  $\omega$  values decreasing with the radial distance ( $\omega = \omega(r)$ , heating from above). Figure 6 presents the critical trajectories of bubbles at four values of the bubble-growth rates, and Figure 7 shows the dependences of calculated values of the fining time,  $\tau_{Fcrit}$ , on the bubble growth rate for the case of angular velocity decreasing with  $r$ . The values of  $\tau_{Fcrit}$  were calculated for the same four values of the initial angular velocity  $\omega_0$  as in the previous case. The positions of the starting points of the critical bubbles proved a similar trend as is presented in Figure 5.

DISCUSSION

The critical starting point of a bubble in a melting space with flow patterns is never located at the bottom of the space, which in fact corresponds to both the theory [9] and calculations [6]. The spiral shape of the function describing the positions of the critical starting points in Figure 5 is a consequence of the common solution of the circular flow and bubble-rise functions. It is known from previous calculations that the small bubble of a constant size ( $\dot{a} = 0$ ) can never reach the glass level in a rotating melt; its starting point would probably be

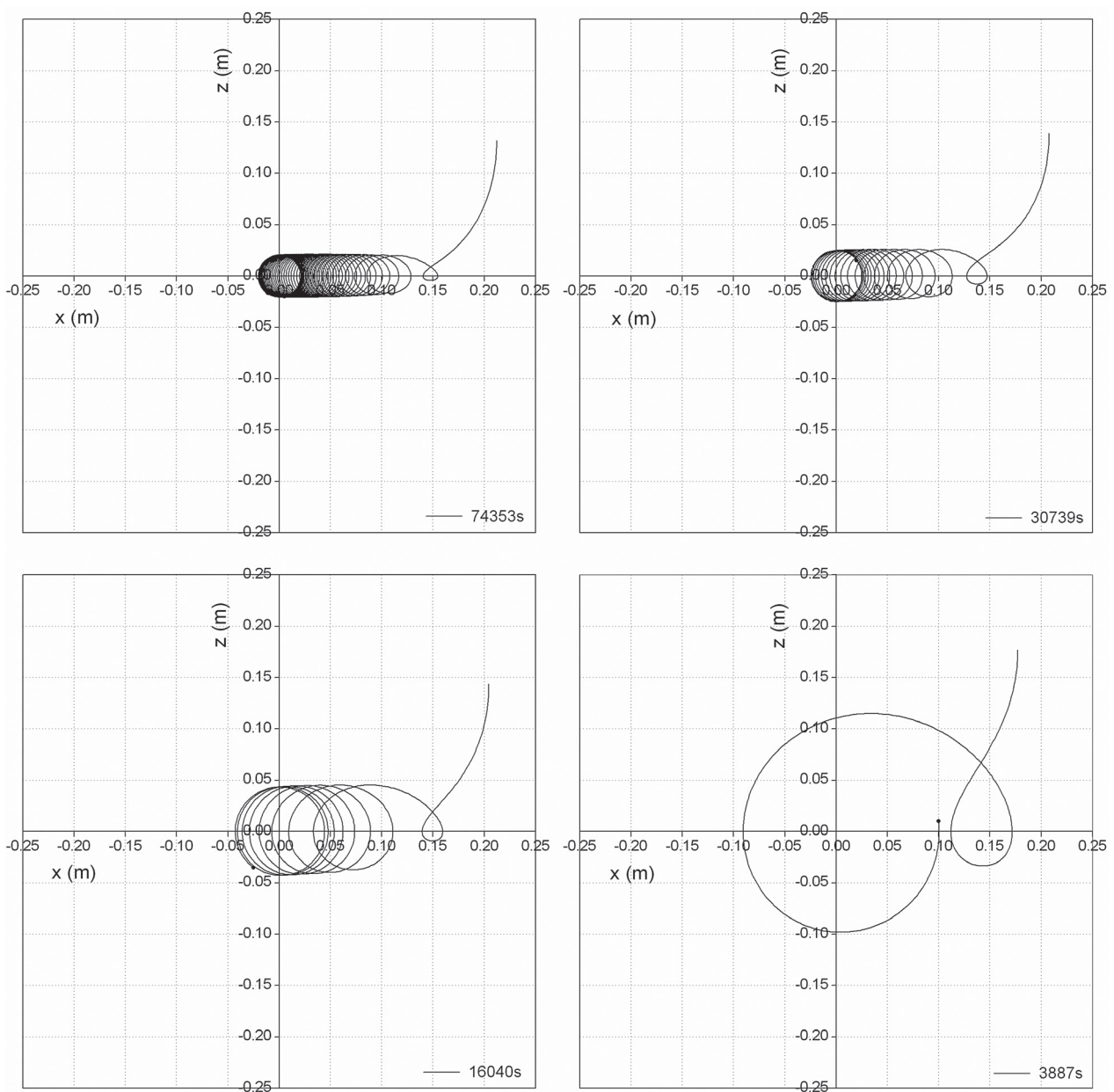


Figure 6. The critical trajectories of bubbles in the circular velocity field of the melt for the bubble-growth rates of  $2 \times 10^{-8}$ ,  $5 \times 10^{-8}$ ,  $1 \times 10^{-7}$  and  $5 \times 10^{-7}$  m/s at  $\omega_0 = 4 \times 10^{-3}$  rad/s in the case of the value of  $\omega$  decreasing with the radius of the space (heating from above).

placed in the centre of the circular flow. As the bubble-growth rate increases, the critical starting point moves from the centre, and the bubble trajectory is characterised by the increasing radius of the spiral (see Figures 3 and 6). Despite the fact that the model is an idealised presentation of the pot furnace, the results presented here provide good qualitative information on the starting points and the shapes of trajectories.

Figures 4 and 7 showing the dependences of the fining times of the critical bubbles on the bubble-growth rates indicate that the shape of the dependence is similar to the case of a quiescent melt ( $\tau_{Fref}$ , see the approximate Equation (2)), so the dependence typifies a power function in the given extent of bubble-growth rates. The proposed semiempirical function of the fining time has the form:

$$\tau_{Fcrit} = \frac{C(\omega)}{\dot{a}^{n(\omega)}} \quad (11)$$

where both  $C$  and  $n$  are constants dependent on the angular velocity  $\omega$ . For the quiescent glass melt applied here, the value of  $C$  is 0.205 and  $n$  is 2/3. The use of the same power function proved to be appropriate for fitting the results of both cases - heating through the wall (the constant value of  $\omega$ ) and heating from above (the value of  $\omega$  decreasing with  $r$ ). For heating through

the wall ( $\omega = k$ ), the values of  $n$  fulfil the condition  $n \in \langle 0.95; 1 \rangle$  and, for heating from above ( $\omega = \omega(r)$ ), the values of  $n$  show slightly lower values,  $n \in \langle 0.95; 0.98 \rangle$ . Generally, the parameter  $n$  increases with growing angular velocity  $\omega$ ; at a higher circulation flow,  $n \rightarrow 1$ , which would fit the hyperbolic dependence. The parameter  $C$  shows a minimum at about  $\omega = 2 \times 10^{-3}$  rad/s. The values of both parameters in the calculations are presented in Table 1.

Figure 8 provides the summarised results in the 3D presentation showing that the values of  $\tau_{Fcrit}$  are lower in the case of heating from above. This is an anticipated result as the bubble rising against the downward flow of the melt is slowed less when the angular velocity gradually decreases with the radius of the rotation of the melt. The impact of the melt angular velocity on the bubble-removal time is seen in Figure 9. The bubble-removal times generally decrease with decreasing melt rotation velocity; nevertheless, the character of the dependence becomes more flattened at higher values of the bubble growth rates. As is evident, the value of  $\tau_{Fcrit}$  becomes almost independent of  $\omega$  when the bubble-growth rate is greater than about  $5 \times 10^{-7}$  m/s. Consequently, in the region of intensive chemical fining, i.e. at relatively high bubble-growth rates, the character of the glass flow has only a minor influence on the fining

Table 1. The values of constants  $n$  and  $C$  as functions of  $\omega_0$ ; the values are valid for cases of both constant values and those decreasing with the radius of the space.

$\omega_0$ (rad/s)	$\omega = k$		$\omega = \omega(r)$	
	C	n	C	n
$1 \times 10^{-3}$	$2.59 \times 10^{-3} \pm 1.7 \times 10^{-4}$	$0.95539 \pm 0.35 \times 10^{-3}$	$3.48 \times 10^{-3} \pm 4.9 \times 10^{-4}$	$0.91842 \pm 7.15 \times 10^{-3}$
$2 \times 10^{-3}$	$2.17 \times 10^{-3} \pm 0.9 \times 10^{-4}$	$0.98468 \pm 2.21 \times 10^{-3}$	$2.32 \times 10^{-3} \pm 2.2 \times 10^{-4}$	$0.95728 \pm 4.86 \times 10^{-3}$
$4 \times 10^{-3}$	$2.70 \times 10^{-3} \pm 0.6 \times 10^{-4}$	$0.99200 \pm 1.29 \times 10^{-3}$	$2.66 \times 10^{-3} \pm 1.8 \times 10^{-4}$	$0.96758 \pm 3.57 \times 10^{-3}$
$1 \times 10^{-2}$	$4.02 \times 10^{-3} \pm 0.3 \times 10^{-4}$	$0.99556 \pm 0.43 \times 10^{-3}$	$3.11 \times 10^{-3} \pm 0.7 \times 10^{-4}$	$0.98351 \pm 1.24 \times 10^{-3}$

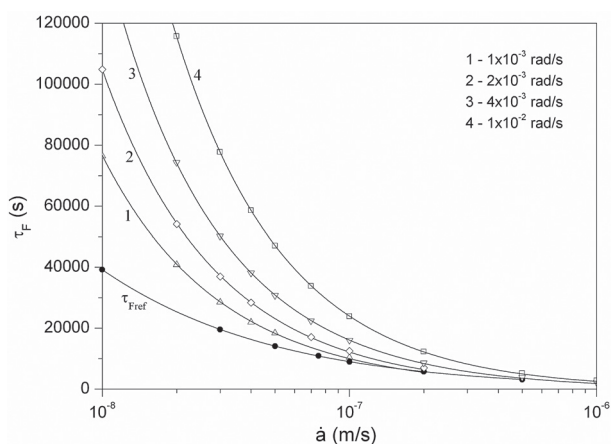


Figure 7. The calculated values of  $\tau_{Fref}$  and  $\tau_{Fcrit}$  for the case of the value of  $\omega$  decreasing with radius (heating from above). The values of  $\tau_{Fcrit}$  were calculated for  $\omega_0 = 1 \times 10^{-3}$ ,  $2 \times 10^{-3}$ ,  $4 \times 10^{-3}$  and  $1 \times 10^{-2}$  rad/s.

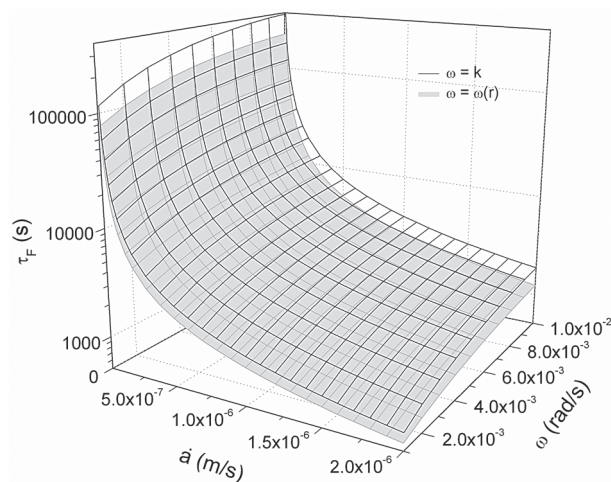


Figure 8. The summarizing dependence of the values of  $\tau_{Fcrit}$  on the bubble growth rate and the initial angular velocity of the melt for cases of both constant and with the radius of the melt rotation decreasing angular velocity.

efficiency. In continuous glass melting, however, the character of the glass flow always distinctly improves or damages the bubble removal process [6, 8]. As is evident from equation (1), the results of bubble modelling may also be presented in terms of the utilisation of the melting space. An illustration of the dependence between  $u$  and the bubble-growth rate is presented in Figure 10. The values of  $u$  for the given initial rotation velocity of the melt and initial bubble radius should go to zero at and approach 1 at high values of  $\dot{a}$ . Figure 10 confirms that the space is almost fully utilised for the bubble-removal process when  $\dot{a} = 10^{-6}$  m/s and higher.

This work presents the application of the simple abstract model to describe the real process, and the question of the quantitative validity of the results is therefore relevant. The proposed model is easy to solve, provides almost instantaneous results yet involves only the principal features of the discontinuous melting process. It follows that some characteristics are not included - e.g. the time-dependent values of the melt angular velocity or the exact relation between the applied temperature gradient and the resulting angular velocity of the melt. The viscosity and density of the model TV glass were applied in this work, but no substantial changes should be expected when using other glass values. Nevertheless, some conclusions will be verified by a numerical modelling.

### CONCLUSION

The following qualitative conclusions may be drawn from the results of the simplified modelling of the discontinuous glass melting (in pot furnaces):

- the fining time of critical bubbles (the smallest bubble demonstrating the maximum time of rising to the glass level) in the vertical rotation field of glass melt

decreases approximately hyperbolically with the increasing bubble-growth rate. The minimum fining time is attained for the quiescent melt. Hence, good chemical fining is significant in both quiescent and rotating melts,

- the fining time of the critical bubbles decreases with the decreasing angular velocity of the melt. The impact of glass-flow character on the fining process becomes negligible at bubble-growth rates higher than about  $5 \times 10^{-7}$  m/s. This value represents the currently achievable value of the bubble-growth rate when applying the appropriate temperature and fining agent,
- the heating of the melt from above with the temperature maximum in the centre of the level shows lower values of fining times in comparison with the case of heating through the wall, where the temperatures are the highest close to the wall,

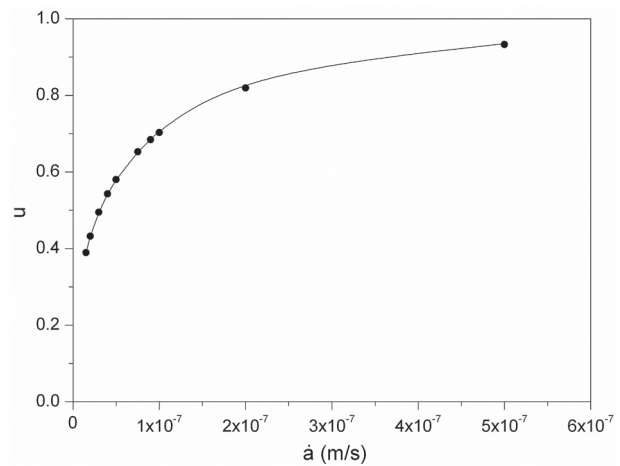


Figure 10. The utilisation of the space for bubble removal against the bubble-growth rate in the case of heating through the wall,  $\omega_0 = 1 \times 10^{-3}$  rad/s.

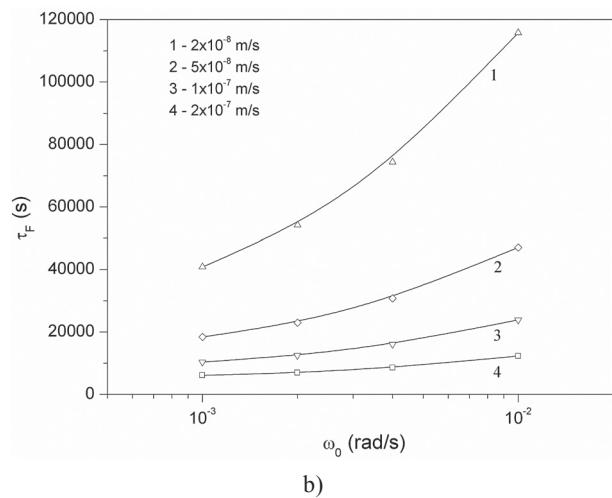
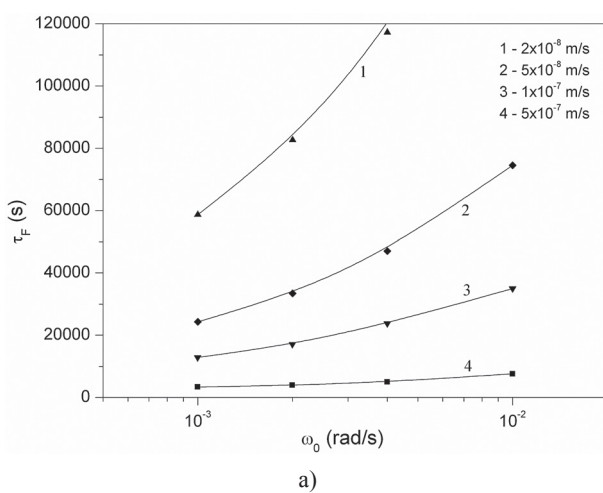


Figure 9. The values of the critical fining time,  $\tau_{Fcrit}$ , as a function of the melt angular velocity,  $\omega$ ; a) The constant value of  $\omega$ , heating through the wall, the bubble-growth rates:  $2 \times 10^{-8}$ ,  $5 \times 10^{-8}$ ,  $1 \times 10^{-7}$  and  $5 \times 10^{-7}$  m/s; b) The value of  $\omega$  decreasing with the radial coordinate, the bubble-growth rates:  $2 \times 10^{-8}$ ,  $5 \times 10^{-8}$ ,  $1 \times 10^{-7}$  and  $2 \times 10^{-7}$  m/s.

- the growing temperature supports both fining and flow intensity. Nevertheless, the increase in fining intensity given by the bubble-growth rate is more relevant for the fining process; therefore, higher temperatures are preferred.

Previous calculations have answered the question of why the relatively large bubbles are observed in the pot furnaces, reaching the glass level even during later stages of the glass fining, although their rising velocity should be very high; the long fining times are caused by their rotation trajectories evoked by natural convection of glass in the pot furnace.

#### Acknowledgement

*This work has been supported by the Technology Agency of the Czech Republic in the project No. TA01010844 "New glasses and their technologies".*

#### References

1. Beerkens R.: *Ceramics-Silikáty* 52, 206 (2008).
2. Balkanli B., Ungan A.: *Glass Technol.* 37, 164 (1996).
3. Matyáš J., Němec L.: *Glass Sci. Technol.* 76, 71 (2003).
4. Němec L., Cincibusová P.: *Ceramics-Silikáty* 49, 286 (2005).
5. Němec L., Jebavá M., Cincibusová P.: *Ceramics-Silikáty* 50, 140 (2006).
6. Němec L., Cincibusová P.: *Ceramics-Silikáty* 52, 240 (2008).
7. Němec L., Cincibusová P.: *Ceramics-Silikáty* 53, 145 (2009).
8. Polák M., Němec L.: *Ceramics-Silikáty* 54, 212 (2010).
9. Cincibusová P.: Ph.D. Thesis, Prague, p. 40 (2010).